Robust Integrated Optimization of Well Placement and Control under Field Production Constraints

Mohammad Salehian, Morteza Haghighat Sefat, Khafiz Muradov

Institute of GeoEnergy Engineering, Heriot-Watt University, Edinburgh EH14 4AS, UK

Abstract

Field development and control optimization aim to maximize the economic profit of oil and gas production while respecting various constraints such as production limits imposed by the available fluid processing capacity and/or reservoir management strategies. The limitations of the existing optimization workflows are 1) well locations or production/injection controls are optimized independently despite the fact that one affects another, and 2) forthcoming field production limits are ignored during at least one of these optimization stages. This paper presents a robust, multi-level framework for field development and control optimization under fluid processing capacity constraints while considering reservoir description uncertainty.

The developed framework is based on sequential iterative optimization of control variables at different levels, where the loop of well placement followed by control optimization continues until no significant improvement is observed in the expected objective value. Simultaneous perturbation stochastic approximation (SPSA) algorithm is employed as the optimizer at all optimization levels. Field production constraints are imposed on the reservoir model using a simplified production network. Smart clustering techniques are applied to systematically select an ensemble of reservoir model realizations as the representative of all available realizations at each optimization level.

The developed framework is tested on the Brugge benchmark field case study with a maximum field liquid production limit imposed via the production network. A comparative analysis is performed for each case to investigate the impact of field liquid production constraints on optimal well placement and control strategy. Results demonstrate that ignoring fluid processing capacity constraints, in one or multiple levels of optimization, results in a sub-optimal scenario, highlighting the significance of the proposed optimization framework in robust field development and management.

Keywords: robust optimization, well placement, optimal control, field production constraints

1. Introduction

Optimization algorithms can be applied to maximize field performance by optimizing one or multiple types of decision variables such as the location of new wells or the control settings of existing production/injection wells while honoring operational constraints. This often results in a high-dimensional, constrained optimization problem with a computationally expensive objective function calculated using a fluid flow simulator. The optimisation should be performed under uncertainty due to limited knowledge of the reservoir performance/geology. An integrated model is further developed to simultaneously capture the flow behavior at subsurface (i.e. in the reservoir and wellbores) as well as surface (i.e. in the production network and processing facilities) and to capture the constraints imposed by any limited processing capacity.

The control variables in this optimization problem can be grouped into 1) integer, model grid cell number-based well locations and 2) continuous well production/injection pressure or rate control settings. In this paper, we refer to optimization on different variable types as different *'optimization levels'* (e.g. the well location optimization is one level, and the well production/injection control optimization is another level). Single-level optimization frameworks were initially developed to optimize only one type of control variables such as well locations (Tavallali et al., 2018) or well control settings (Nikolaou et al., 2006; Codas et al., 2012). These were later extended to multi-level optimization (e.g. for optimizing the drilling order, well type, location, and control settings) that

This is a peer-reviewed, accepted author manuscript of the following article: Salehian, M., Sefat, M. H., & Muradov, K. (2021). Robust integrated optimization of well placement and control under field production constraints. Journal of Petroleum Science and Engineering, 205, [108926]. https://doi.org/10.1016/ j.petrol.2021.108926

accounts for correlations between the levels during the optimization process. Current multi-level approaches can be classified into two groups: (1) *joint optimization* (Bellout et al., 2012; Shirangi et al., 2018; Lu and Reynolds, 2019): this approach simultaneously optimizes a single augmented vector containing all control variables from different levels. However, one may not be able to achieve an optimal solution when using this approach in full-field applications due to the large number of control variables (Lu et al., 2017a). (2) *sequential optimization* (Li et al., 2013; Forouzanfar et al., 2016; Lu et al., 2017a): in this approach, the main problem is divided into sub-problems with a reduced number of control variables. Each sub-problem is a single-level optimization with a single type of control variable. The field design is iteratively optimized as a sequence of such sub-problems (in order to capture the correlation among the values of control variables in optimal scenarios) and the loop is terminated when no major improvement is observed in the objective value (Li and Jafarpour, 2012). Lu et al. (2017a) compared the iterative sequential method with the joint method in well placement and control optimization problems using an approximate-gradient-based algorithm. Better performance was achieved using the iterative sequential approach mainly due to the lower quality of the gradient in the joint method with a single augmented vector of control variables of different types (i.e. discrete well locations and continuous control settings).

Both single-level and joint optimization approaches have previously been applied to problems with production constraints. Epelle and Gerogiorgis (2019) used an integrated model of a reservoir and production system to optimize water injection rates in a synthetic case and achieved a higher net present value (NPV) due to the improved sweep efficiency. Any other production settings (e.g. liquid production rate, well bottom-hole pressures) or well locations were fixed. Tavallali and Karimi (2016) used the joint method to simultaneously optimize well placement and control settings in a synthetic reservoir model using a heuristic search optimization method, which increased the economic profit of the optimum case. As for the sequential approach: so far it has been used only in subsurface optimization problems without considering the production network (Li et al., 2013; Forouzanfar et al., 2016; Lu et al., 2017a; Salehian et al., 2020a).

An integrated, field development model is normally created by coupling the surface network with the subsurface reservoir models in order to provide a realistic performance of the whole system as well as to capture the production constraints. These integrated field models can be developed using commercial simulators or approximation methods. The integrated modeling approaches available in commercial reservoir simulators can be classified as 1) implicit with sub-models (i.e. of the reservoir, well, surface network and processing system) all modeled within a single simulator [e.g. Tavallali et al. (2018) using ECLIPSE] or 2) explicit in which detailed sub-models are developed in individual simulators following by sequentially solving them using an integration framework [e.g. as in Orioha et al. (2012) using Integrated Production Modeling (IPM) or in Taha et al. (2013) using Integrated Asset Modeler (IAM)]. The implicit approach has the advantage of creating fast, simplified, and mathematically stable integrated models, while the explicit approach can create potentially more detailed sub-models. Nevertheless, optimisation using a detailed, full-scale, integrated field model simulated using commercial simulators normally becomes computationally very expensive. To address this issue, approximation techniques are employed in various optimization studies to provide a faster and reasonably representative model of the integrated system as an alternative to the commercial simulators. Gunnerud and Foss (2010) and Gunnerud et al. (2012) used piecewise linear approximation methods to create simple, fast, integrated models for oil production. Gupta and Grossmann (2012), Kosmidis et al. (2005), and Tavallali et al. (2014) employed Mixed-Integer Nonlinear Programming (MINLP) to develop a problem-specific formulation for both subsurface and surface flow dynamics followed by simultaneous optimization of well locations, surface facility capacity expansions, and production/injection scenarios. Epelle and Gerogiorgis (2019) coupled a subsurface commercial simulator with a surrogate-based surface facility model and achieved an improved accuracy by adaptively updating the surrogate model during the optimization process. The generated approximated models have the advantage of less computation time as compared to commercial simulators; however, they can become excessively complicated or unrepresentative in real fields with a large number of wells attached to a processing facility via an often-complex network (Li et al., 2012).

Current field development optimization workflows can be further classified into three main groups based on the employed optimization algorithm: (1) stochastic derivative-free and metaheuristic algorithms such as the genetic algorithm (Almeida et al., 2010; Lu and Reynolds, 2020; Ma and Leung, 2020) or the particle swarm optimization algorithm (Panahli, 2017; Ding et al., 2020), (2) adjoint gradient-based algorithms (Van Essen et al., 2011; Kahrobaei et al., 2013; Bukshtynov et al., 2015; Farajzadeh et al., 2019), and (3) stochastic approximated gradient-based algorithms such as the Simultaneous Perturbation Stochastic Approximation (SPSA) (Spall, 1992) or the Stochastic Simplex Approximate Gradient (StoSAG) methods (Fonseca et al., 2017; Liu and Reynolds, 2020). The stochastic derivative-free and metaheuristic algorithms have the advantage of the global search for the optimal solution from all types of control variables (e.g. categorical, integer, or continuous variables). However, they typically require a high number of function evaluations, and their performance is degraded rapidly with increasing the number of control variables (Zingg et al., 2008). The adjoint gradient-based methods are computationally attractive. However, access to the reservoir simulation source code is required to calculate the gradient, which makes them impractical for use with commercial (black box) simulators. The approximate gradient-based algorithms overcome the above issues by stochastically estimating the gradient of a black-box objective function using a reasonably sized ensemble of simultaneous perturbations of control variables, where an ensemble of less than 10 perturbations per iterations can usually provide a good balance between the gradient accuracy and computation time (Haghighat Sefat et al., 2016; Salehian et al., 2020b). These algorithms have been successfully employed to solve large-scale well placement [e.g. Jesmani et al. (2016) using SPSA] and well control problems [e.g. Haghighat Sefat et al. (2016) using SPSA and Lu et al. (2017b) using StoSAG].

Tens to hundreds of reservoir model realizations are often developed to represent the model's underlying uncertainty due to the limited reservoir description knowledge. A robust, optimal well placement/control solution ideally should be obtained by optimizing the expected value of the objective function over the ensemble of all model realizations. Instead, several techniques have been developed to select a relatively small ensemble of model realizations to represent all the realizations in order to reduce the computational demand associated with the robust optimization process. One simple realization selection technique is the random sampling method (Chen et al., 2012), which cannot guarantee to capture the underlying uncertainty existing in all available realizations. Iteratively updating the randomly selected ensembles during the optimization process (e.g. Jesmani et al. (2020)) is another method that can potentially alleviate this problem, especially when the number of iterations is large. A systematic approach is to tailor the realization selection process to the objective of the subsequent optimization (Wang et al., 2012; Haghighat Sefat et al., 2016; Salehian et al., 2020b). Wang et al. (2012) recommended projecting all model realizations to two-dimensional space while each dimension is selected from static (e.g. permeability, oil-water contact) or temporal (e.g. cumulative oil production) property of the model considering the subsequent optimisation objectives. Haghighat Sefat et al. (2016) showed that the realization selection at the well control optimization level is best supported by considering the area between well/zonal water cut curves as a similarity/dissimilarity measure when projecting all model realizations to two-dimensional space. Both approaches will be followed by clustering and selecting representative realizations from each cluster.

This paper presents a multi-level framework for well placement and control optimization under fluid processing capacity constraints (e.g. due to a production facility with limited capacity, or a production sharing agreement among multiple operators, or a tie-back throughput capacity to an existing facility, etc.). The iterative sequential optimization method (Li and Jafarpour, 2012) is employed to optimize well placement and control settings iteratively, and this loop continues until no significant improvement in the expected objective values is observed. SPSA is used as the optimizer based on its superior performance compared to alternative derivative-free algorithms such as PSO/GA (Spall et al.,

2006) as well as following its recent successful applications in large-scale problems (Li et al., 2013; Pouladi et al., 2020; Salehian et al., 2020a). Commercial simulator ECLIPSE (Schlumberger, 2017) has been used to model multiphase flow through the integrated system consisting of both the reservoir and the production network. Fit-for-purpose clustering procedures are employed to systematically select a small ensemble of reservoir model realizations to efficiently capture the underlying model uncertainties at each optimization level. The proposed approach has been tested on a representative benchmark case study, known as the Brugge field model, to investigate the impact of production constraints on the optimal field development solutions.

The outline of this paper is as follows: First, problem formulation for robust well placement/control optimization under production constraints, with an uncertain reservoir model, is presented. Next, the benchmark case study (Brugge oil field model) and the reservoir model with imposed field production constraints are presented. The developed framework is then applied to the benchmark case study, considering both the deterministic (single realization) and the probabilistic (multiple realizations) reservoir model, followed by a discussion of the results, and conclusions.

2. Problem formulation

The objective is to maximize a field's Net Present Value (NPV) over its expected production life. Assuming a fixed number of wells to drill, each solution is of approximately the same capital expenditure (i.e. CAPEX or investment). Hence the incremental NPV used to compare solutions in this study only considers the cash flow due to the oil and water production. Given a reservoir model m, the NPV function is given by

$$\underset{\substack{x\in\mathbb{R}^{N_x}\\ m\in\mathbb{R}^{N_m}}}{J}(x,m)=\sum_{n=1}^{S}\left\{\left[\sum_{j=1}^{N_P}\left(r_o q_{o,j}^n - r_{pw} q_{w,j}^n\right)-\sum_{k=1}^{N_I}\left(c_{wi} q_{wi,k}^n\right)\right]\times\frac{\delta t^n}{(1+b)^{t_n}}\right\} \tag{1}$$

where x is the vector of the control variables, m is the vector of the uncertain reservoir description properties, n is the n^{th} time step of the reservoir simulation, S is the total number of simulation steps, δt^n is the length of n^{th} simulation step, t_n is the simulation time at the end of the n^{th} time step, b is the annual discount rate in decimal, and N_P and N_I are the number of producers and injectors, respectively. The cost coefficients r_o, r_{pw}, and c_{wi} denote the oil price, the produced water handling cost, and the water injection cost, respectively; all in (USD/STB). $q_{o,j}^n$ and $q_{w,j}^n$ are the oil and water production rates of well j at time step n in STB/day. $q_{wi,k}^n$ is the water injection rate of well k at time step n in STB/day. To take the geological uncertainty into account, the expected NPV (J_E) over an ensemble of reservoir model realizations is maximized at each robust optimization level. The robust optimization problem at each level is defined by

$$\max_{x\in\mathbb{R}^{N_x}} J_E(x)=\frac{1}{N_e}\sum_{k=1}^{N_e} J(x,m_k) \tag{2}$$

$$subject\ to\ x_i^{min}\le x_i\le x_i^{max}\ , i=1\ ,2\ ,\dots,N_x \tag{3}$$

where N_e denotes the number of representative reservoir model realizations; $m_k, k=1,2,\dots,N_e$ represents the vector of k^{th} reservoir model parameters (e.g. porosity and permeability fields, fault transmissibility, oil-water contacts); and x_i^{min} and x_i^{max} are the lower and upper bound for the i^{th} component of the control variable vector, respectively.

Table 1 shows the economic values used for NPV calculation. Eq. (4) is employed to scale the control variables (x) from the original domain $[x_{min}\ ,x_{max}]$ to [0, 1] to eliminate the impact of different ranges of control variables at both well placement and control optimization levels.

$$u_i = \frac{x_i - x_i^{min}}{x_i^{max} - x_i^{min}} \tag{4}$$

Table 1-Economic parameters for calculating NPV

Symbol	Parameter	Value
r_o	Oil Price	50 USD/STB
r_{pw}	Water production cost	6 USD/STB
c_{wi}	Water injection cost	3 USD/STB
b	Discount rate	10 %/year

Simulation runs are conducted using the commercial simulator to calculate the objective function for the specified set of control variables and model realizations. The production constraints are implicitly imposed through the simulator following Forouzanfar et al. (2013); Volkov and Bellout (2017); Beykal et al. (2018). SPSA (Spall, 1992) is used as the optimization algorithm at all levels. The number of iterations at well placement and control optimization levels is set to 150 and 300, respectively. The convergence of the SPSA algorithm depends on the tuning parameters α_k and c_k, which define the size of the increment in the state vector and the derivative's differential vector at iteration k. Spall (1998) suggested the following decaying sequences to calculate α_k and c_k to ensure a gradually refining search:

$$\alpha_k = \frac{a}{(\mathbb{A} + k + 1)^{\vartheta}} \tag{5}$$

$$c_k = \frac{c}{(k+1)^{\gamma}} \tag{6}$$

where a, c, $\mathbb{A}$, ϑ, and γ are positive, real numbers. The values of ϑ and γ are recommended to be 0.602 and 0.101 (Spall, 1992). The stability constant, $\mathbb{A}$, is recommended to be 5-10% of the expected, or allowed, number of iterations when optimizing continuous variables (Spall, 2005). Jesmani et al. (2020) recommended using a larger $\mathbb{A}$ (e.g. $\mathbb{A}$ was set to 100 that is 33.3% of the 300 iterations) to achieve a more refined search to enhance the convergence of the algorithm in well placement optimization problems with discrete control variables. In this work, $\mathbb{A} = 100$ and $\mathbb{A} = 10$ is used for well placement and well control optimization levels, respectively. Haghighat Sefat et al. (2016) recommended setting $0.1 \leq \alpha_0 \leq 0.5$ and c_{min} (i.e. when $k = k_{max}$) between 0.025 and 0.1 based on the complexity of the search space. Initial sensitivity analysis in this work showed that more stable search process and faster convergence is achieved when $\alpha_0 = 0.5$ and $c_{min} = 0.08$ for both well location and control optimization. Detailed information about SPSA formulation for well placement and control optimization can be found in Salehian et al. (2020a). The following constraints are applied to control variables during each optimization level:

At the well location optimization level:

- A minimum inter-well distance constraint of $200\ m$ (equivalent to 2 grid blocks) is imposed using the penalty method following Lu et al. (2017a).
- Well locations are maintained within the actual, irregular reservoir boundary limits, represented by a binary matrix with 0 and 1 elements indicating null and active reservoir grids, respectively. Following Salehian et al. (2020a), each well is moved to the nearest active grid if it appears outside the reservoir boundaries during location optimization.

At the well control optimization level:

- Following Brugge field's production constraints provided by Peters et al. (2010) and Peters et al. (2013), the producers are all controlled by the Bottom Hole Pressure (BHP) varying between 725 and 1595 psi, while the injectors are controlled by the well water injection rate varying between 0 and 6289 STB/day.
- The producers are shut when their water cut exceeds 90% (i.e. when they stop being profitable as calculated using Table 1 economic parameters).

The production network with limited fluid processing capacity is simulated by assigning a maximum constraint on the total liquid production rate from all producers in the model. More information on the reservoir model and production network is provided in section 3.

2.1. Realization selection and clustering

Selecting a small ensemble of model realizations as the representative of all available realizations can significantly reduce the computation time of robust optimization. A systematic approach is to tailor the realization selection process to the objective of the subsequent optimization level. Wang et al. (2012) proposed projecting all model realizations to two-dimensional space while each dimension attributes to a temporal (e.g. cumulative oil production) or static (e.g. permeability, oil-water contact, original oil in place) property of the model, followed by clustering and selecting representative realizations from each cluster. They used the normalized oil-water contact and the cumulative oil production as model attributes when selecting representative realizations for well location optimization to maximize NPV by enhancing reservoir sweep efficiency. Haghighat Sefat et al. (2016) used the pairwise distance between water cut curves of all model realizations as the similarity/dissimilarity measure when selecting realizations for well production optimization to increase oil production by delaying the water breakthrough. Shirangi and Durlofsky (2016) also proposed to measure similarity/dissimilarity between model realizations using a low-dimensional feature vector containing a combination of static (e.g. permeability, grid dimensions, original oil in place) and dynamic (varying with time) (e.g. cumulative oil/water production) model properties, tailored to the optimization objectives. They found that both static and dynamic model properties need to be considered when selecting realizations for well location optimization, while dynamic properties become especially crucial in realization selection for well control optimization.

Well placement optimization: Following Wang et al. (2012), the realization selection at the well placement optimization level is performed by creating a two-dimensional map where each model realization is characterized by its normalized permeability distance and the area under the field's cumulative oil production curve. The normalized permeability distance is defined as the Euclidean distance between the permeability field of a particular realization (m_i) and the average permeability field over all available realizations ($\overline{m}$) (i.e., $d_i = \|m_i - \overline{m}\|_2$ where $\|.\|$ represents the l_2-norm). K-means clustering (Seber, 2009) is then performed to group all available realizations (n_r) into a small number of clusters (n_c) by iteratively finding the optimal cluster centers, i.e. $\tau_{opt} = \{\tau_1, \tau_2, \dots, \tau_{n_c}\}$, such that the summation of the distances of all n_r realizations from the nearest cluster center is minimized. Each realization is then assigned to the nearest cluster center (Scheidt and Caers, 2009; Haghighat Sefat et al., 2016). Determining the optimum number of clusters is an ill-posed problem and mostly involves some form of intuition supported by a performance measure. The Silhouette value (Rousseeuw, 1987) evaluates how well a data point is assigned to a particular cluster and is used as the clustering performance measure in this work. Assuming n_c clusters:

$$Sil_i = \frac{b_i - a_i}{\max(a_i, b_i)} \tag{7}$$

$$a_i = d_{i,C(i)} \text{ and } b_i = \min_{C \neq C(i)} d_{i,C} \tag{8}$$

$$d_{i,C} = \frac{1}{\#\, data\ points\ in\ cluster\ C} \sum_{l \epsilon C} D(u_i, u_l) \tag{9}$$

$$\overline{Sil}(n_c) = \frac{1}{n_r} \sum_{i=1,\ldots,n_r} Sil_i \tag{10}$$

where Sil_i is the Silhouette value for data point i, $D(u_i, u_l)$ is the Euclidean distance between data point i and data point l, $d_{i,C}$ shows the average dissimilarity of data point i with all other data points in cluster C. Hence a_i indicates the average dissimilarity of data point i with all other data points within the same cluster while b_i shows the lowest average dissimilarity of point i with any point in any other cluster (i.e. the neighboring cluster, which is the next best fit for point i). The optimum number of clusters ($n_{c_{opt}}$) is then determined by comparing the average silhouette values ($\overline{Sil}(n_c)$) for different numbers of clusters (n_c), where the maximum silhouette value indicates the best quality of clustering.

Well control optimization: The objective of the well control optimization level in this study is to improve oil recovery, which is generally achieved by delaying early water breakthrough in wells. Hence, following Haghighat Sefat et al. (2016), the realization selection at the well control optimization level is best supported by calculating a pairwise distance between the area under well water cut curves of all model realizations as their difference measure , given by:

$$D(m_i, m_j) = \sum_{g=1}^{n_p} \int_{t=0}^{t_f} \left(f_{wc_g}(m_i, t) - f_{wc_g}(m_j, t) \right) dt \tag{11}$$

where $f_{wc_g}(m_i, t)$ is the water cut in the g^{th} production well as a response of model i (m_i) at time t, n_p is the total number of production wells, and t_f is the final production time. The $n_r \times n_r$ dissimilarity matrix is then projected into two-dimensional space using multidimensional scaling (MDS) (Borg and Groenen, 2003), preserving the Euclidean distance between data points in 2D as close as possible to the distance measured in the original space (Eq. (11)). K-means clustering followed by average silhouette value analysis is then performed to group model realizations into $n_{c_{opt}}$ clusters, similar to the routine followed at the well placement optimization level.

Following Scheidt and Caers (2009) and Haghighat Sefat et al. (2016), the realization closest to the center of each cluster is selected as the representative of that cluster at both optimization levels. Figure 1 shows the flow diagram of the proposed robust, integrated optimization framework with well placement and control settings as the optimization levels.

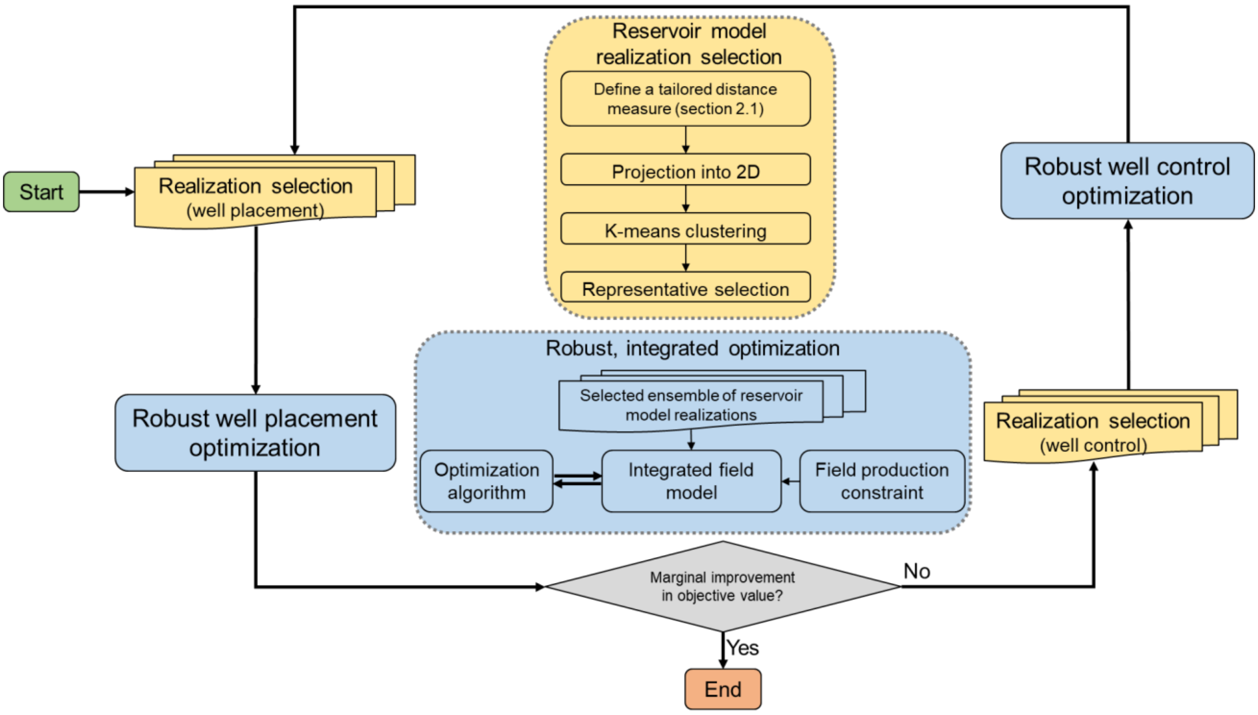

Figure 1-Flow diagram of the proposed robust, integrated optimization framework.

3. Model description

3.1. Reservoir model

The Brugge model is a publicly available benchmark reservoir model, consisting of 139 × 48 × 9 (total of 60,048) grid blocks with a relatively heterogeneous permeability distribution (Chen et al., 2010). The reservoir model contains oil and water only. The original model consists of 20 producers and 10 injectors. Five vertical producers and five vertical injectors are kept from the original model in this work, due to the limited computational resources. All wells are vertical and completed in all nine reservoir layers. The total production time is set to 30 years. Figure 2 shows the top structure of the model with the base case well locations. The uncertainty in the model description is quantified by 104 equiprobable realizations of the permeability, porosity, and net-to-gross (NTG) value distribution (Peters et al., 2013). More information on the reservoir rock and fluid properties of the Brugge model can be found in Peters et al. (2010). The top (i, j) location coordinates of the wells are optimized during the well location optimization level, which results in $10 \times 2 = 20$ control variables. It is assumed that all wells are completed and operational at time zero, i.e. no drilling/completion sequence has been cosniderd. 30 control steps (of 1 year each) are considered during the well production/injection optimization level resulting in the total of $30 \times 10 = 300$ control variables.

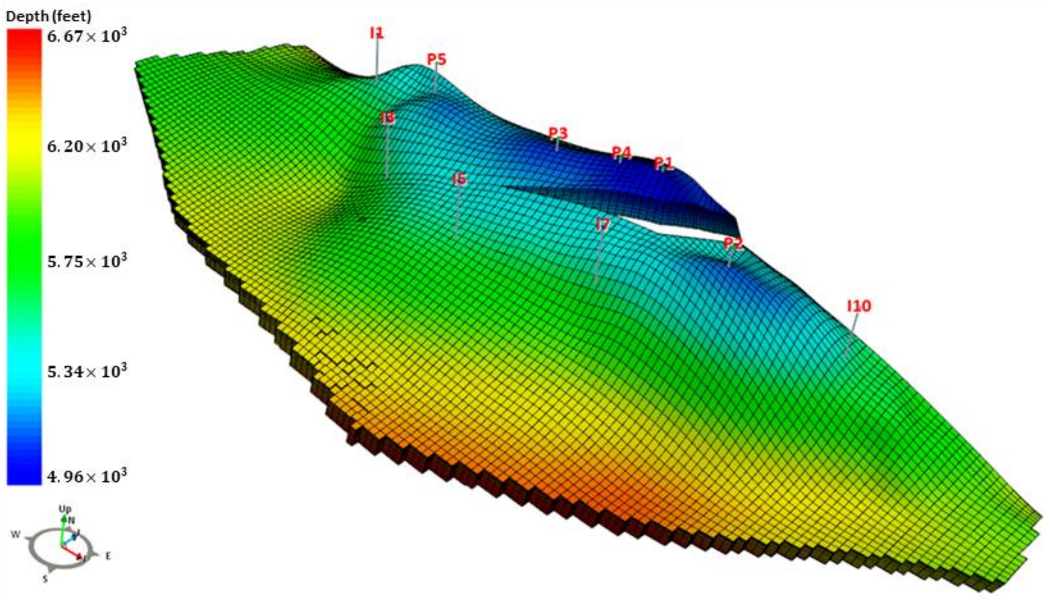

Figure 2- Top structure of the Brugge model.

3.2. Production Network

The NETWORK option in ECLIPSE reservoir simulator is used to develop connect a simple production network to the Brugge reservoir model (Figure 3). This keyword uses a multi-level grouping hierarchy technique to connect a group of wells to a manifold and a pipeline network, which directs the production stream towards the parent group. The parent group gathers the production from one or multiple manifolds and directs it along another pipeline to its own parent group. This hierarchy continues until a sink with a fixed pressure (i.e. separator or stock tank) is encountered. The simulator implicitly solves the multiphase flow in the reservoir and dynamically balances the flow rates and pressure losses within the network. More information is available in the ECLIPSE user manual (Schlumberger, 2017).

The production network used in this study consists of producers and injectors groups and is shown in Figure 3. For simplicity, it is assumed that the produced gas volume, as well as the pressure losses in all pipelines, are negligible. The limited production capacity is simulated by assigning a liquid production rate constraint on the production manifold (where it affects all producers in that group).

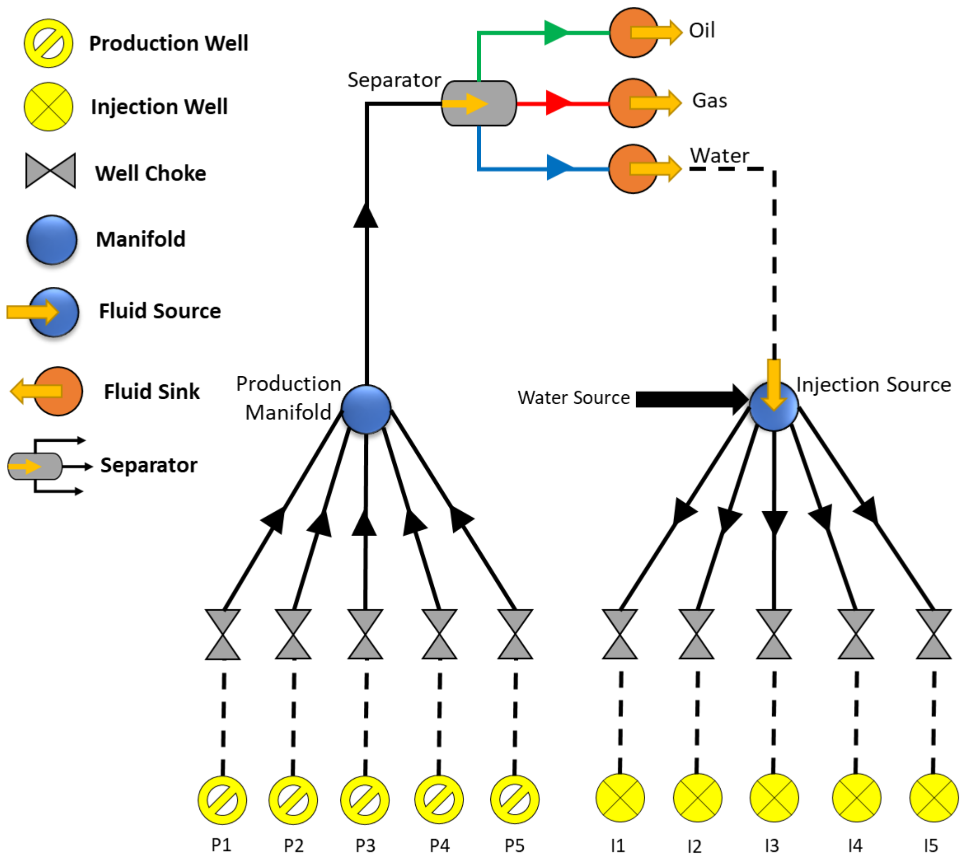

Figure 3-Schematic representation of the reservoir model and production system for the Brugge field.

4. Results and discussions

Well locations and control settings of the Brugge model are optimized considering both deterministic (i.e. a single reservoir model realization is used, no uncertainty is assumed) and probabilistic (104 equiprobable reservoir model realizations) scenarios. The following cases with the allocated maximum FLPR (Field Liquid Production Rate) constraints are considered:

1- Case 1: No FLPR constraint (FLPR reaches almost 65,000 STB/day at the highest level)
2- Case 2: Maximum FLPR = 40,000 STB/day (named as “40K”)
3- Case 3: Maximum FLPR = 30,000 STB/day (named as “30K”)
4- Case 4: Maximum FLPR = 20,000 STB/day (named as “20K”)

Note that the optimization cases with FLPR limits (cases 2-4) are referred to as “constrained optimization” cases, while case 1 is referred to as “unconstrained optimization” in this paper.

4.1. Deterministic optimization of well placement and control

A single, most likely reservoir model realization, corresponding to $P50$ recovery calculated based on the initial well locations and base case (i.e. max production and injection) well control settings, of the Brugge model is selected. Figure 4 shows improvement in the NPV during 100 iterations of the well placement optimization level under the allocated FLPR constraints. The observed oscillations in NPV are due to imposing the minimum inter-well distance constraint as a penalty term in the objective function definition (see Lu et al. (2017a) for the penalty term formulation). Figure 5 shows the optimal well placement solutions corresponding to four different FLPR constraints. A more restrictive production constraint results in locating producers at high permeability regions with more scattered injectors located further away from the producers to improve sweep efficiency by increasing oil production potential and delaying water breakthrough.

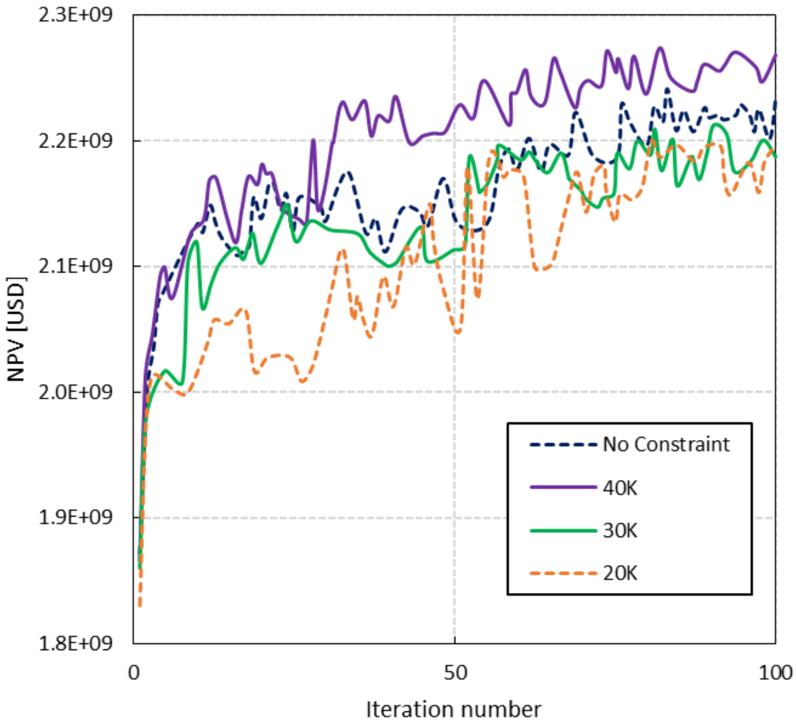

Figure 4 – Objective value (NPV) during well placement optimization under different FLPR constraints.

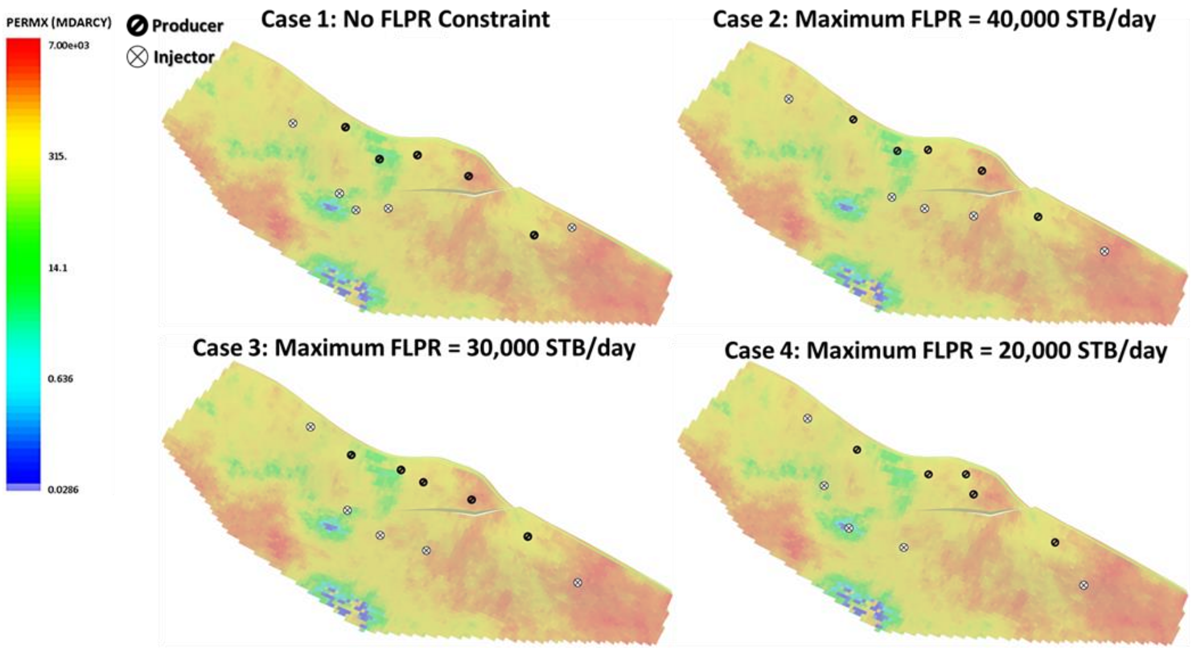

Figure 5 – Optimal well locations under different FLPR constraints.

Table 2 compares the objective values for three well placement optimization strategies under the allocated production constraints:

Row 1 - Base case: No well location optimization (i.e. initial well locations).
Row 2 - W_1: Single optimal well location scenario is obtained while ignoring the production constraints
Row 3 - W_2: Optimal well locations are calculated for each individual scenario while considering the corresponding production constraints during the optimization procedure.

Comparing rows 2 (W_1) and 3 (W_2) of Table 2 shows that ignoring production constraints during well placement optimization stage can result in a sub-optimal development scenario. Row 4 in Table 2 shows improvement with respect to the base case for constrained optimization scenarios indicating the greater importance of well placement optimization for cases with lower fluid processing capacity to ensure that more oil and less water is produced within the limited capacity. A slightly higher NPV is obtained in the optimal scenario for the "40K" case ($2.27 \times 10^9\ USD$) as compared to the unconstrained case ($2.24 \times 10^9\ USD$) indicating that prioritizing production from wells with low oil production potential, to respect the allocated production constraint, acts as some form of well control optimization and inherently enhances the sweep efficiency.

Table 2 – Objective values (1) of the base case; (2) obtained by unconstrained well location optimization; (3) obtained by constrained well location optimization; and their percent change w.r.t. to the base case.

		Maximum FLPR (STB/day)			
		No constraint	40,000	30,000	20,000
		$NPV \times 10^9\ (USD)$			
1	Base case	1.86	1.78	1.68	1.53
2	W_1	2.24	2.24	2.19	2.16
3	W_2	−	2.27	2.21	2.20
4	% improvement w.r.t. base case	+20.4	+27.6	+31.5	+43.8

The control settings for each optimal well location solution are then individually optimized at the next optimization level. Figure 6 shows the improvement in NPV of the four cases with various production constraints as a result of well control optimization for the corresponding optimal well location solution. The sequential optimization loop was then terminated since no further improvements in NPV were achieved in the well location optimization level of the second loop.

The delayed recovery due to the imposed production limit is shown in Figure 7 (note that in the base case, the initial well locations and the fully open well control scenario with no FLPR constraint are selected), however, the recovery efficiency of the constrained cases can approach that of the unconstrained one by applying an optimal control to optimally located well. A different behavior might be observed for a different reservoir type (e.g. a compartmentalized reservoir with sealing faults and/or naturally fractured reservoir). The optimal control scenario generated by the optimization framework can be analyzed by engineers to provide insights into the optimal control strategy for a particular reservoir. This shows the importance of an efficient integrated optimization framework to support decision making in field development and control planning. Table 3 compares the objective values for different well placement and control strategies under fluid production constraints:

Row 1 – W_1: Production rate constraints are considered during well locations optimization level – no well control optimization is performed (i.e. fully open control).
Row 2 – W_1C_1: Single optimal well location and control scenario obtained while ignoring the production constraints during both optimization levels.
Row 3 – W_1C_2: Production constraints are ignored during well location optimization but considered during well control optimization.

Row 4 – W_2C_2: Production rate constraints are considered during both well location and well control optimization levels.

Comparing row 1 (W_1) with the other three ones shows that control optimization results in an added value, regardless of considering production constraints. However, ignoring production constraints at one (W_1C_2) or multiple (W_1C_1) levels of optimization would result in a sub-optimal scenario, i.e. in a lower objective value as compared to the case of constrained optimization at all levels (W_2C_2). Figure 8 and Figure 9 show the BHPs and the water injection rates for the optimal scenarios, respectively. Figure 10 compares the impact of well location and control optimization under various production rate constraints (i.e. W_2 and W_2C_2 in Table 2 and Table 3, respectively). Note that here the production rate constraints are explicitly considered during both well location and control optimization levels. Prioritizing production from wells with low oil production potential, to respect the field production rate constraint, inherently acts as some form of optimal control, reducing the added value from well control optimization level in cases with restricted field production. This increases the impact of the optimal well location to ensure that maximum oil and minimum water is produced within the limited capacity. On the other side, the cases with higher production constraints experience earlier water breakthrough which increases the added value of well control optimization.

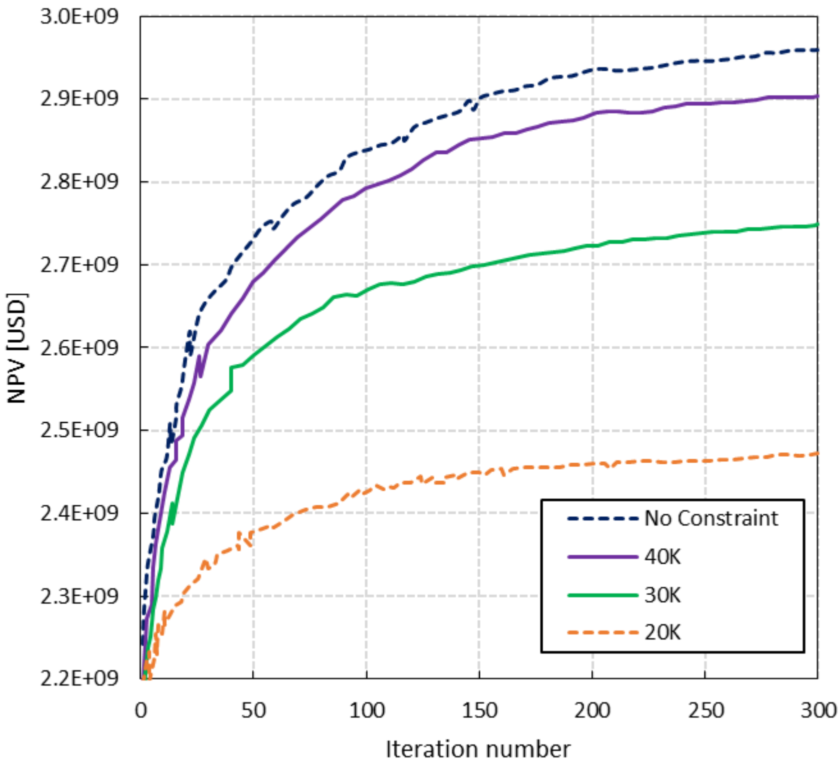

Figure 6 - Objective value of during well control optimization under different FLPR constraints.

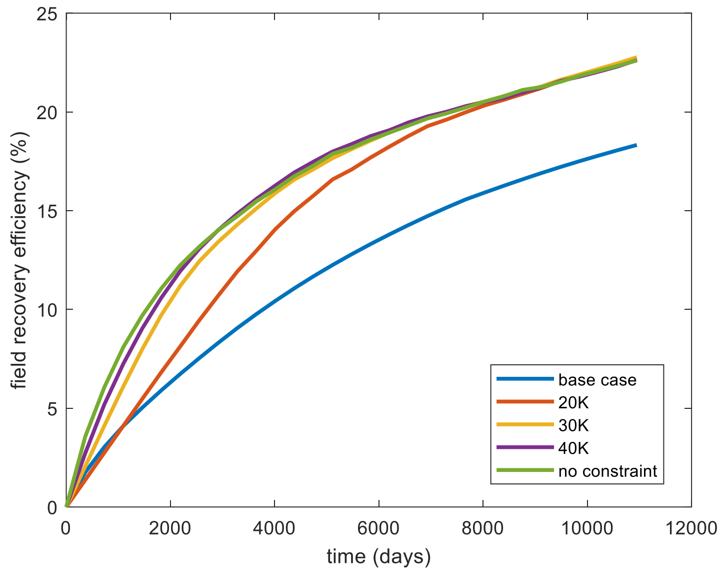

Figure 7 – Field recovery efficiency after well placement and control optimization under different FLPR constraints and the base case.

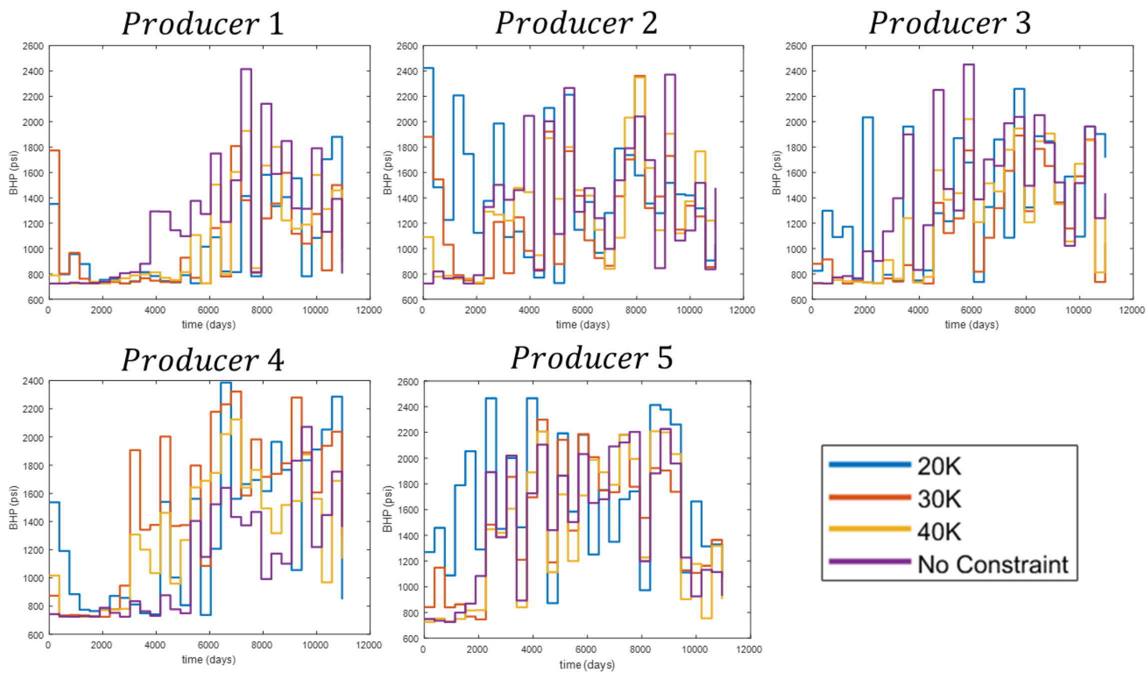

Figure 8 – Optimal BHP values based on optimal well locations under different FLPR constraints. Production rate constraints are considered during both well location and well control optimization levels.

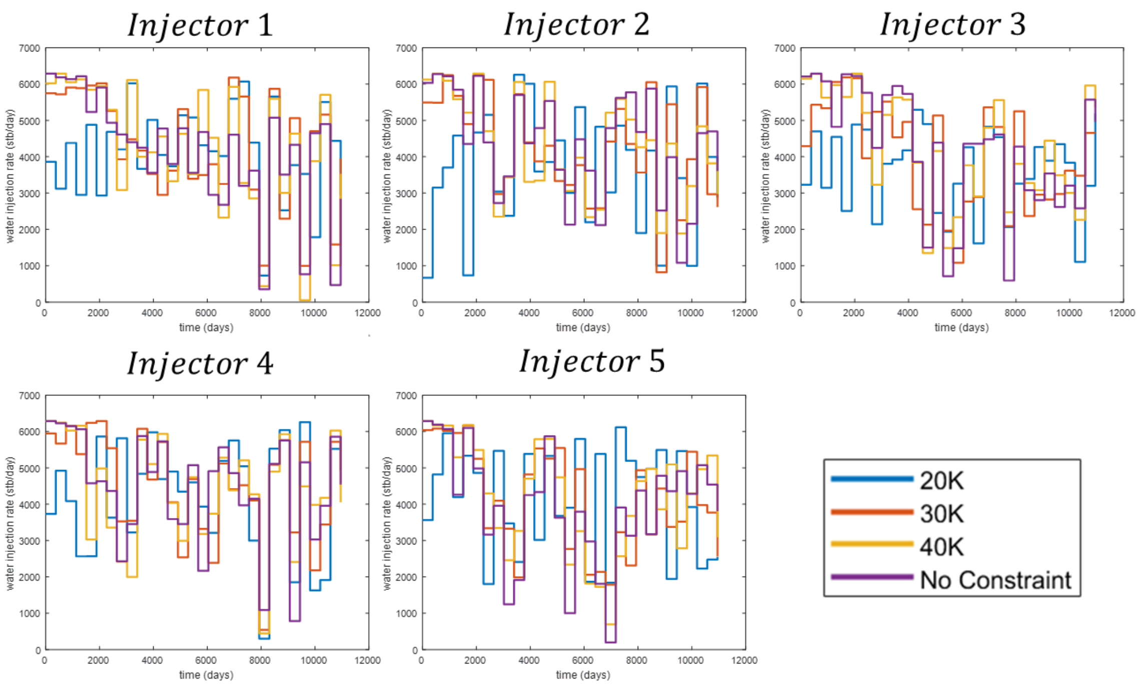

Figure 9 – Optimal water injection rates based on optimal well locations under different FLPR constraints. Production rate constraints are considered during both well location and well control optimization levels.

Table 3 – Objective values obtained by (1) constrained well location optimization with no control optimization (same as row 3 in Table 2) (2) unconstrained well location and control optimization (3) unconstrained well location optimization and constrained control optimization (4) constrained well location and control optimization, and the percent change as a result of control optimization.

		Maximum FLPR (STB/day)			
		No constraint	40,000	30,000	20,000
		$NPV \times 10^9$ (USD)			
1	W_1	2.24	2.27	2.21	2.20
2	W_1C_1	2.96	2.87	2.71	2.32
3	W_1C_2	–	2.89	2.73	2.43
4	W_2C_2	–	2.90	2.75	2.47
	%improvement w.r.t. fully open scenario (W_1)	+32.1	+27.7	+24.4	+10.4

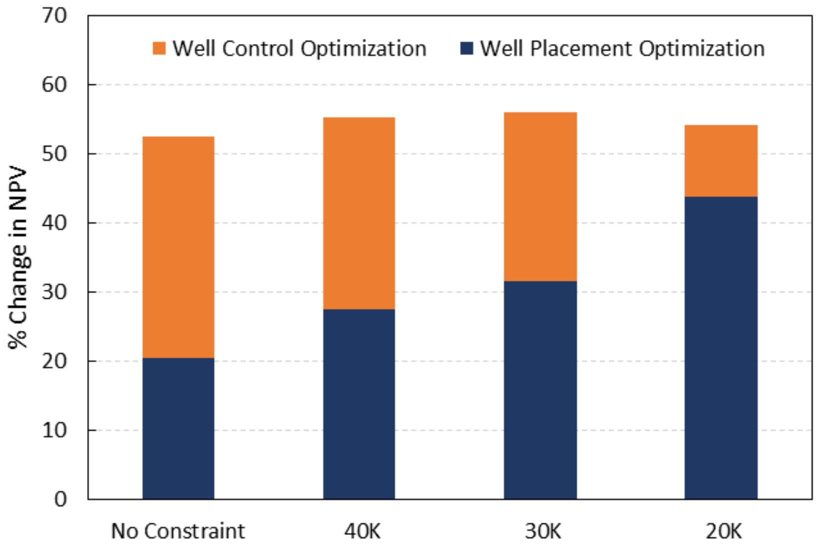

Figure 10-The improvement in objective value as a result of well placement and control optimization for four cases under different FLPR constraints.

4.2. Robust optimization of well placement and control

This section extends the study to robust well placement and control optimization over an ensemble of realizations of the Brugge model under assigned fluid production capacity constraints. All model realizations are projected in 2D using the normalized permeability distance and the cumulative oil production (cacluated based on the initial well locations and base case, fully open control scenario) as distance measures calculated for each case with different production rate constraints (Figure 11). The optimum number of clusters is then identified based on the average Silhouette analysis for each case (Figure 12), which is found to be four ($n_{c_{opt}} = 4$) and five ($n_{c_{opt}} = 5$) for the unconstrained and constrained cases, respectively. The realization closest to the center of each cluster is selected as the cluster representative (Figure 11), to be employed during the robust well location optimization level.

Figure 13 shows the improvement in the expected NPV of the selected realizations during well placement optimization iterations for each case. Table 4 shows the $E(NPV)$ over all realizations for three well placement optimization strategies, similar to those of Table 2 in the deterministic example. Comparing rows 2 and 3 of Table 4 shows that ignoring production constraints during the well placement optimization level results in a sub-optimal development scenario. Row 4 in Table 4 shows the improvement with respect to the base case after the well placement optimization stage, indicating the greater importance of this level for cases with stricter production constraints to ensure more oil and less water production within a limited fluid processing capacity. However, despite the deterministic example, no inherent enhancement in sweep efficiency of constrained cases is observed after considering reservoir uncertainty during the optimization process, since the amount of improvement in sweep efficiency significantly varies with different model properties (i.e. different model realizations).

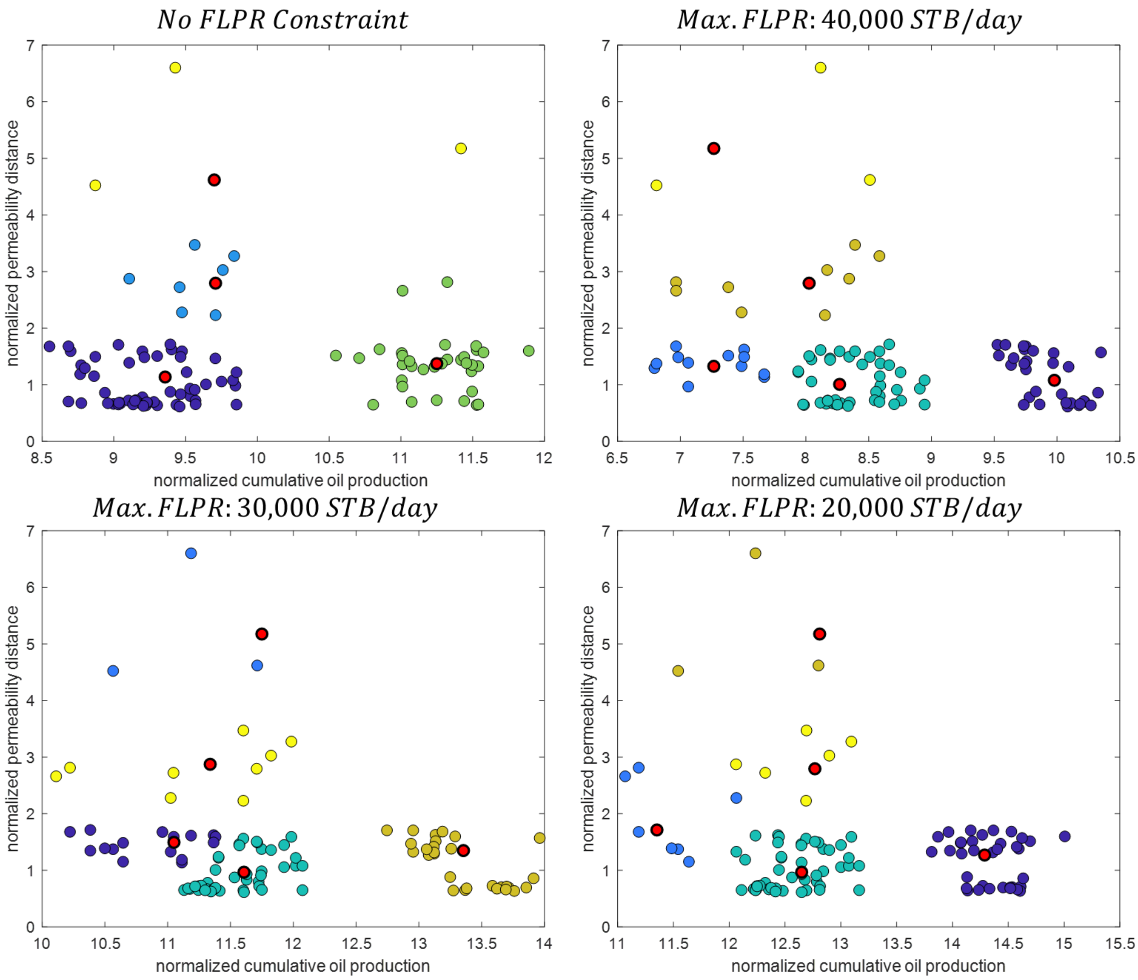

Figure 11 – K-means clustering of reservoir model realizations under different FLPR constraints, considering the optimum number of clusters, prior to well placement optimization. Red points show the cluster representatives.

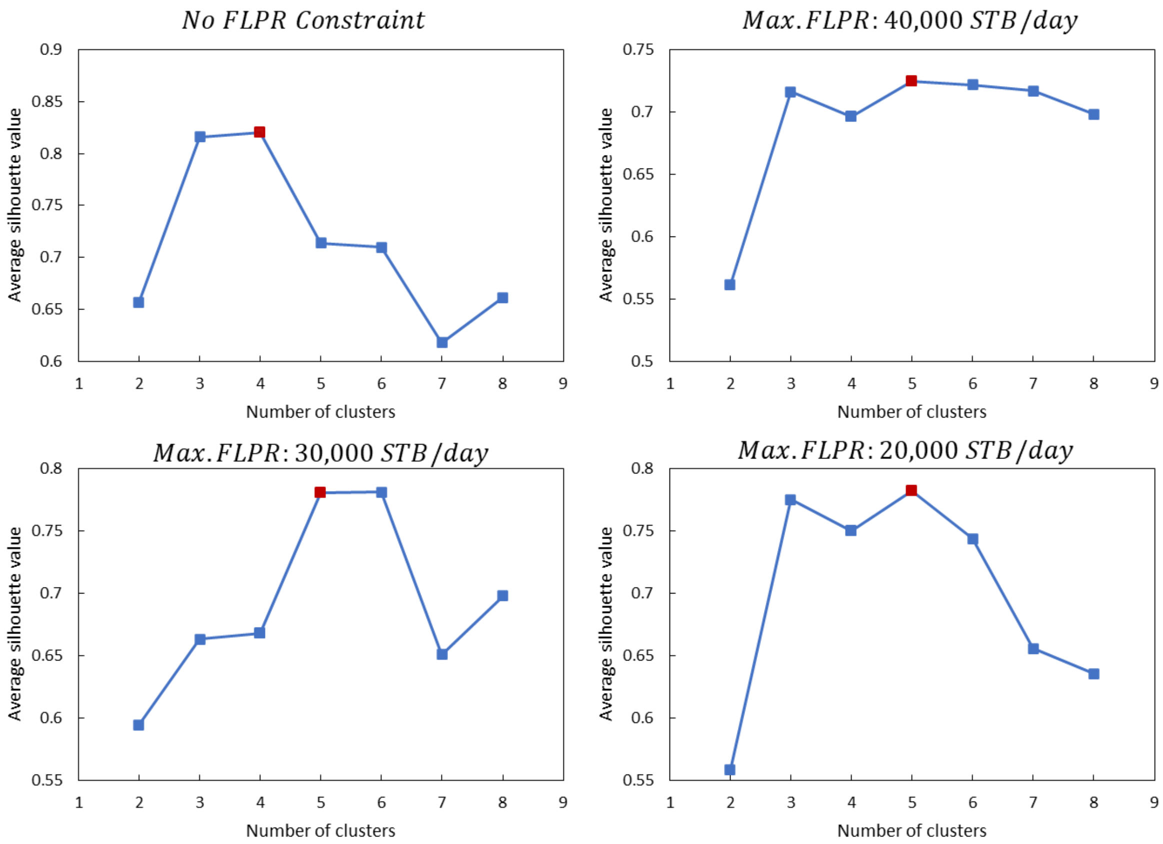

Figure 12 – Average Silhouette value of all data points for different number of clusters in k-means.

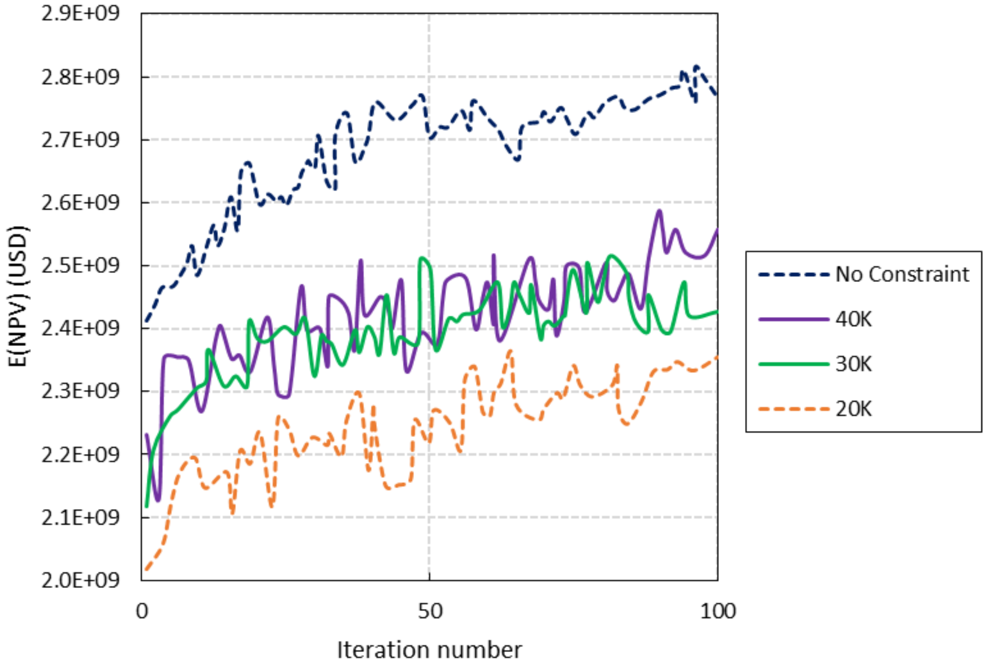

Figure 13 – E(NPV) of the corresponding ensemble of realizations during well placement optimization under different FLPR constraints.

Table 4 – Mean objective values (over all realizations) (1) of the base case (2) obtained by unconstrained robust well placement optimization (3) obtained by constrained robust well placement optimization, and the percent change w.r.t. to the base case. "R" denotes the robust optimization.

	Maximum FLPR (STB/day)			
	No constraint	$40{,}000$	$30{,}000$	$20{,}000$
	$E(NPV) \times 10^9$			
1 Base Case	1.93	1.79	1.74	1.61
2 Unconstrained robust well location optimization ($R.W_1$)	2.31	2.27	2.28	2.13
3 Constrained robust well location optimization ($R.W_2$)	$-$	2.30	2.29	2.17
4 %improvement w.r.t. base case as	$+19.7$	$+28.5$	$+32.2$	$+34.8$

The distance measure described in Eq.(11) is used to project all model realizations into 2D using the optimal well locations obtained under the corresponding FLPR constraints. Figure 14 shows the clustering performance, where the optimum number of clusters is determined using average Silhouette value analysis for each case. The closest realizations to cluster centers are selected as the representative realizations to be used during the robust well control optimization level. Figure 15 shows the improvement in $E(NPV)$ of the selected ensemble of reservoir model realizations during 300 iterations of well control optimization.

Table 5 compares the expected objective values for different well placement and control strategies, similar to those of Table 3 in the deterministic example. A trend similar to that of deterministic example can be observed in the robust optimization case, where ignoring production constraints at one (row 3) or both (row 2) levels of optimization has resulted in a sub-optimal scenario, degrading the expected value of the objective function as compared to row 4 (i.e. considering constraints at both levels). Figure 16 compares the impact of robust well placement and control optimization under various field production rate constraints (i.e. $R.W_2$ and $R.W_2C_2$ in Table 4 and Table 5, respectively). Similar to the deterministic example, the impact of the optimal well location is higher in cases with restricted field production. However, the earlier water breakthrough in cases with higher production capacities increases the added value of the well control optimization.

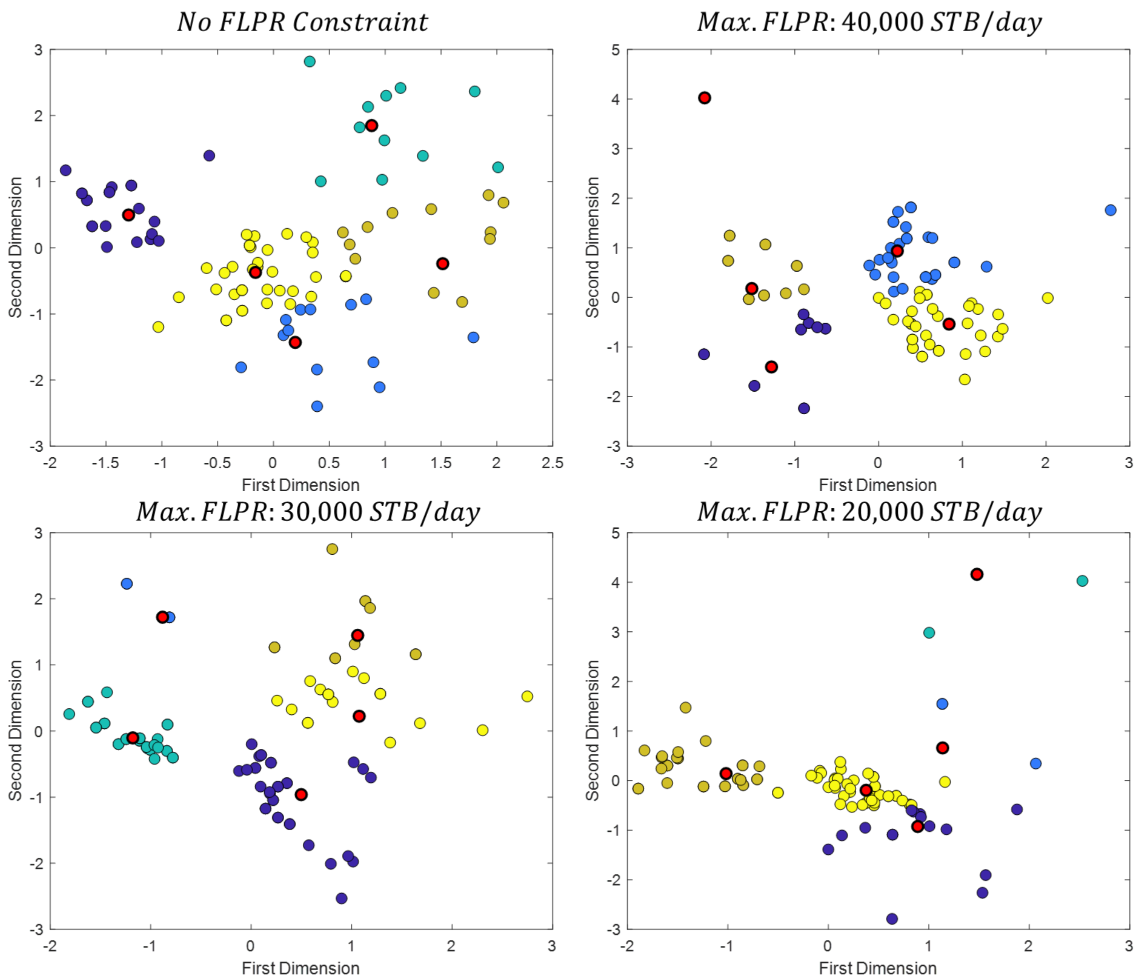

Figure 14 – K-means clustering for reservoir model realization selection under different FLPR constraints prior to well control optimization. Red points show the cluster representatives.

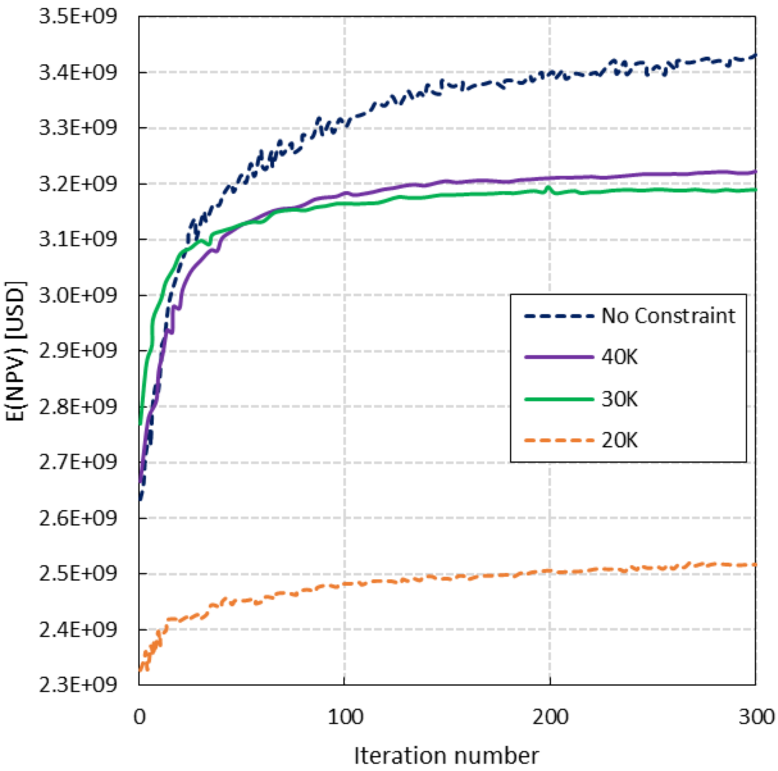

Figure 15 – E(NPV) of the corresponding ensemble of reservoir model realizations during well control optimization under different FLPR constraints.

Table 5 – Mean objective values (over all realizations) obtained by (1) constrained well location optimization with no control optimization (same as row 3 in Table 4) (2) unconstrained well location and control optimization (3) unconstrained well location optimization and constrained control optimization (4) constrained well location and control optimization, and the percent change as a result of control optimization. "R" denotes the robust optimization.

	Maximum FLPR (STB/day)			
	No constraint	40,000	30,000	20,000
	$E(NPV) \times 10^9$			
1 $R.W_1$	2.31	2.30	2.29	2.17
2 $R.W_1C_1$	2.95	2.84	2.73	2.28
3 $R.W_1C_2$	–	2.89	2.74	2.31
4 $R.W_2C_2$	–	2.91	2.76	2.43
%improvement w.r.t. fully open scenario ($R.W_1$)	+27.7	+26.5	+20.0	+12.0

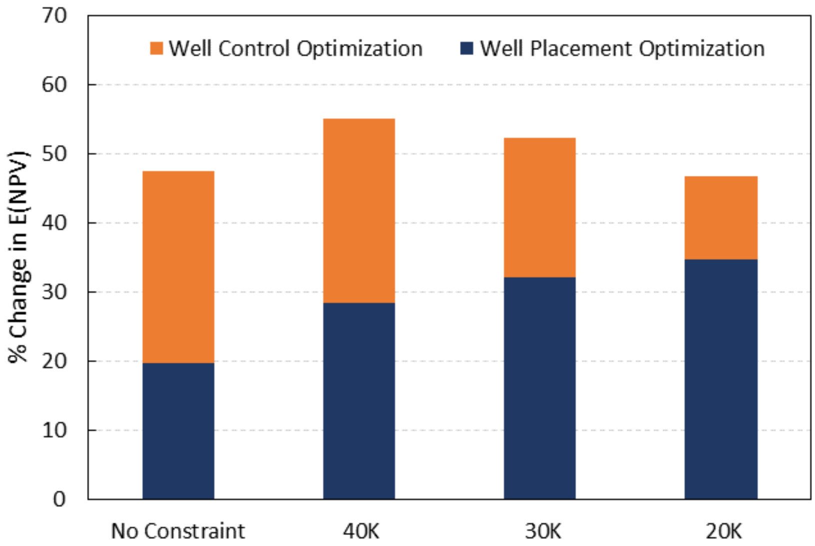

Figure 16- The improvement in expected objective value (over all realizations) as a result of robust well placement and control optimization for four cases under the allocated FLPR constraints.

5. Summary and Conclusions

This study presented an integrated, multi-level optimization framework to provide novel insights into the impact of field production constraints on optimal well placement and control. The proposed framework was applied to a representative benchmark case study while field production constraints were imposed on the reservoir model using a simplified production network. Well placement and control settings were optimized under various field fluid processing capacities, considering deterministic and probabilistic scenarios. Smart clustering techniques, tailored to the objective of subsequent optimization level, were used to systematically select an ensemble of representative reservoir model realizations in the robust optimization problem. SPSA algorithm was employed as the optimizer while the developed framework is compatible with other optimization algorithms as well.

Results show that ignoring field production constraints in one or multiple levels of the optimization process would result in sub-optimal scenarios, highlighting the significance of integrated optimization in robust field development and control. A more restrictive field production constraint resulted in locating producers at high permeability regions with more scattered injectors locating further away from producers to enhance the sweep efficiency by increasing the chance of oil production and delaying the water breakthrough. Prioritizing production from wells with low oil production potential, to respect the field production rate constraint, inherently acts as some form of optimal control by allowing them to produce longer and therefore to bring their reserves-depletion success closer to that of the wells with higher productivity. Hence, lower added value is obtained from the well control optimization level in the cases with restricted field production. As a result, this increases the relative impact of the well location optimisation. On the contrary, the cases with higher production constraints experience earlier water breakthrough which increases the added value of well control optimization.

6. Acknowledgments

Authors are thankful to the sponsors of the "Value from Advanced Wells II (VAWE II)" Joint Industry Project at Heriot-Watt University for providing financial support, and to Schlumberger for allowing academic access to their software.

References

Almeida, L.F., Vellasco, M.M. and Pacheco, M.A., 2010. Optimization system for valve control in intelligent wells under uncertainties. Journal of Petroleum Science and Engineering, 73(1-2): 129-140.

Bellout, M.C., Ciaurri, D.E., Durlofsky, L.J., Foss, B. and Kleppe, J., 2012. Joint optimization of oil well placement and controls. Computational Geosciences, 16(4): 1061-1079.

Beykal, B. et al., 2018. Global optimization of grey-box computational systems using surrogate functions and application to highly constrained oil-field operations. Computers & Chemical Engineering, 114: 99-110.

Borg, I. and Groenen, P., 2003. Modern multidimensional scaling: Theory and applications. Journal of Educational Measurement, 40(3): 277-280.

Bukshtynov, V., Volkov, O., Durlofsky, L.J. and Aziz, K., 2015. Comprehensive framework for gradient-based optimization in closed-loop reservoir management. Computational Geosciences, 19(4): 877-897.

Chen, C., Li, G. and Reynolds, A., 2012. Robust constrained optimization of short-and long-term net present value for closed-loop reservoir management. SPE Journal, 17(03): 849-864.

Chen, C., Wang, Y., Li, G. and Reynolds, A.C., 2010. Closed-loop reservoir management on the Brugge test case. Computational Geosciences, 14(4): 691-703.

Codas, A., Campos, S., Camponogara, E., Gunnerud, V. and Sunjerga, S., 2012. Integrated production optimization of oil fields with pressure and routing constraints: The Urucu field. Computers & Chemical Engineering, 46: 178-189.

Ding, S., Lu, R., Xi, Y., Liu, G. and Ma, J., 2020. Efficient well placement optimization coupling hybrid objective function with particle swarm optimization algorithm. Applied Soft Computing, 95: 106511.

Epelle, E.I. and Gerogiorgis, D.I., 2019. Optimal rate allocation for production and injection wells in an oil and gas field for enhanced profitability. AIChE Journal, 65(6).

Farajzadeh, R., Kahrobaei, S., De Zwart, A. and Boersma, D., 2019. Life-cycle production optimization of hydrocarbon fields: thermoeconomics perspective. Sustainable Energy & Fuels, 3(11): 3050-3060.

Fonseca, R.R.M., Chen, B., Jansen, J.D. and Reynolds, A., 2017. A stochastic simplex approximate gradient (StoSAG) for optimization under uncertainty. International Journal for Numerical Methods in Engineering, 109(13): 1756-1776.

Forouzanfar, F., Della Rossa, E., Russo, R. and Reynolds, A.C., 2013. Life-cycle production optimization of an oil field with an adjoint-based gradient approach. Journal of Petroleum Science and Engineering, 112: 351-358.

Forouzanfar, F., Poquioma, W.E. and Reynolds, A.C., 2016. Simultaneous and sequential estimation of optimal placement and controls of wells with a covariance matrix adaptation algorithm. SPE Journal, 21(02): 501-521.

Gunnerud, V. and Foss, B., 2010. Oil production optimization—A piecewise linear model, solved with two decomposition strategies. Computers & Chemical Engineering, 34(11): 1803-1812.

Gunnerud, V., Foss, B.A., McKinnon, K. and Nygreen, B., 2012. Oil production optimization solved by piecewise linearization in a Branch & Price framework. Computers & Operations Research, 39(11): 2469-2477.

Gupta, V. and Grossmann, I.E., 2012. An efficient multiperiod MINLP model for optimal planning of offshore oil and gas field infrastructure. Industrial & Engineering Chemistry Research, 51(19): 6823-6840.

Haghighat Sefat, M., Elsheikh, A.H., Muradov, K.M. and Davies, D.R., 2016. Reservoir uncertainty tolerant, proactive control of intelligent wells. Computational Geosciences, 20(3): 655-676.

Jesmani, M., Jafarpour, B., Bellout, M., Hanea, R. and Foss, B., 2016. Application of simultaneous perturbation stochastic approximation to well placement optimization under uncertainty, ECMOR XV-15th European Conference on the Mathematics of Oil Recovery. European Association of Geoscientists & Engineers, pp. cp-494-00133.

Jesmani, M., Jafarpour, B., Bellout, M.C. and Foss, B., 2020. A reduced random sampling strategy for fast robust well placement optimization. Journal of Petroleum Science and Engineering, 184: 106414.

Kahrobaei, S., Van Essen, G., Van Doren, J., Van den Hof, P. and Jansen, J., 2013. Adjoint-based history matching of structural models using production and time-lapse seismic data, SPE Reservoir Simulation Symposium. Society of Petroleum Engineers.

Kosmidis, V.D., Perkins, J.D. and Pistikopoulos, E.N., 2005. A mixed integer optimization formulation for the well scheduling problem on petroleum fields. Computers & Chemical Engineering, 29(7): 1523-1541.

Li, J., Misener, R. and Floudas, C.A., 2012. Continuous-time modeling and global optimization approach for scheduling of crude oil operations. AIChE Journal, 58(1): 205-226.

Li, L. and Jafarpour, B., 2012. A variable-control well placement optimization for improved reservoir development. Computational Geosciences, 16(4): 871-889.

Li, L., Jafarpour, B. and Mohammad-Khaninezhad, M.R., 2013. A simultaneous perturbation stochastic approximation algorithm for coupled well placement and control optimization under geologic uncertainty. Computational Geosciences, 17(1): 167-188.

Liu, Z. and Reynolds, A.C., 2020. A Sequential-Quadratic-Programming-Filter Algorithm with a Modified Stochastic Gradient for Robust Life-Cycle Optimization Problems with Nonlinear State Constraints. SPE Journal.

Lu, R., Forouzanfar, F. and Reynolds, A.C., 2017a. Bi-objective optimization of well placement and controls using stosag, SPE Reservoir Simulation Conference. Society of Petroleum Engineers.

Lu, R., Forouzanfar, F. and Reynolds, A.C., 2017b. An efficient adaptive algorithm for robust control optimization using StoSAG. Journal of Petroleum Science and Engineering, 159: 314-330.

Lu, R. and Reynolds, A., 2019. Joint Optimization of Well Locations, Types, Drilling Order and Controls Given a Set of Potential Drilling Paths, SPE Reservoir Simulation Conference. Society of Petroleum Engineers.

Lu, R. and Reynolds, A.C., 2020. Joint Optimization of Well Locations, Types, Drilling Order, and Controls Given a Set of Potential Drilling Paths. SPE Journal.

Ma, Z. and Leung, J.Y., 2020. Design of warm solvent injection processes for heterogeneous heavy oil reservoirs: A hybrid workflow of multi-objective optimization and proxy models. Journal of Petroleum Science and Engineering: 107186.

Nikolaou, M., Cullick, A.S. and Saputelli, L.A., 2006. Production Optimization: A Moving-Horizon Approach, Intelligent Energy Conference and Exhibition. Society of Petroleum Engineers.

Orioha, H.I., Gruba, C.J., Muoneke, G. and Ezuka, I.O., 2012. Application of IPM Modeling for Production Surveillance, Allocation and Optimization, SPE International Production and Operations Conference & Exhibition. Society of Petroleum Engineers.

Panahli, C., 2017. Implementation of Particle Swarm Optimization Algorithm within FieldOpt Optimization Framework-Application of the algorithm to well placement optimization, NTNU.

Peters, E., Chen, Y., Leeuwenburgh, O. and Oliver, D., 2013. Extended Brugge benchmark case for history matching and water flooding optimization. Computers & Geosciences, 50: 16-24.

Peters, L. et al., 2010. Results of the Brugge benchmark study for flooding optimization and history matching. SPE Reservoir Evaluation & Engineering, 13(03): 391-405.

Pouladi, B. et al., 2020. Enhancement of SPSA algorithm performance using reservoir quality maps: Application to coupled well placement and control optimization problems. Journal of Petroleum Science and Engineering: 106984.

Rousseeuw, P.J., 1987. Silhouettes: a graphical aid to the interpretation and validation of cluster analysis. Journal of computational and applied mathematics, 20: 53-65.

Salehian, M., Haghighat Sefat, M. and Muradov, K., 2020a. A Multi-Solution Optimization Framework for Well Placement and Control SPE Reservoir Evaluation & Engineering.

Salehian, M., Haghighat Sefat, M. and Muradov, K., 2020b. A Robust Multi-Solution Framework for Well Location and Control Optimization, ECMOR XVII - 17th European Conference on the Mathematics of Oil Recovery. European Association of Geoscientists and Engineers, Edinburgh, United Kingdom.

Scheidt, C. and Caers, J., 2009. Uncertainty quantification in reservoir performance using distances and kernel methods--application to a west africa deepwater turbidite reservoir. SPE Journal, 14(04): 680-692.

Schlumberger, 2017. ECLIPSE® User Manual.

Seber, G.A., 2009. Multivariate observations, 252. John Wiley & Sons.

Shirangi, M.G. and Durlofsky, L.J., 2016. A general method to select representative models for decision making and optimization under uncertainty. Computers & geosciences, 96: 109-123.

Shirangi, M.G., Volkov, O. and Durlofsky, L.J., 2018. Joint optimization of economic project life and well controls. SPE Journal, 23(02): 482-497.

Spall, J.C., 1992. Multivariate stochastic approximation using a simultaneous perturbation gradient approximation. IEEE transactions on automatic control, 37(3): 332-341.

Spall, J.C., 1998. Implementation of the simultaneous perturbation algorithm for stochastic optimization. IEEE Transactions on aerospace and electronic systems, 34(3): 817-823.

Spall, J.C., 2005. Introduction to stochastic search and optimization: estimation, simulation, and control, 65. John Wiley & Sons.

Spall, J.C., Hill, S.D. and Stark, D.R., 2006. Theoretical framework for comparing several stochastic optimization approaches, Probabilistic and Randomized Methods for Design under Uncertainty. Springer, pp. 99-117.

Taha, M. et al., 2013. Effective exploitation of tight gas reservoirs using Integrated Asset Modelling (IAM) approach, SPE/PAPG Annual Technical Conference. Society of Petroleum Engineers.

Tavallali, M., Karimi, I., Halim, A., Baxendale, D. and Teo, K., 2014. Well placement, infrastructure design, facility allocation, and production planning in multireservoir oil fields with surface facility networks. Industrial & Engineering Chemistry Research, 53(27): 11033-11049.

Tavallali, M.S., Bakhtazma, F., Meymandpour, A. and Karimi, I.A., 2018. Optimal Drilling Planning by Considering the Subsurface Dynamics–Combing the Flexibilities of Modeling and a Reservoir Simulator. Industrial & Engineering Chemistry Research.

Tavallali, M.S. and Karimi, I.A., 2016. Integrated oil-field management: from well placement and planning to production scheduling. Industrial & Engineering Chemistry Research, 55(4): 978-994.

Van Essen, G., Van den Hof, P. and Jansen, J.-D., 2011. Hierarchical long-term and short-term production optimization. SPE Journal, 16(01): 191-199.

Volkov, O. and Bellout, M.C., 2017. Gradient-based production optimization with simulation-based economic constraints. Computational Geosciences, 21(5-6): 1385-1402.

Wang, H., Echeverría-Ciaurri, D., Durlofsky, L. and Cominelli, A., 2012. Optimal well placement under uncertainty using a retrospective optimization framework. Spe Journal, 17(01): 112-121.

Zingg, D.W., Nemec, M. and Pulliam, T.H., 2008. A comparative evaluation of genetic and gradient-based algorithms applied to aerodynamic optimization. European Journal of Computational Mechanics/Revue Européenne de Mécanique Numérique, 17(1-2): 103-126.